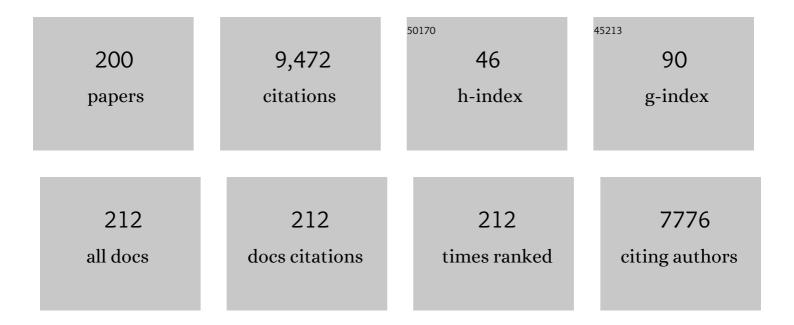
List of Publications by Year in descending order

Source: https://exaly.com/author-pdf/4842706/publications.pdf Version: 2024-02-01



#	Article	IF	CITATIONS
1	Purely organic electroluminescent material realizing 100% conversion from electricity to light. Nature Communications, 2015, 6, 8476.	5.8	799
2	Efficient Persistent Room Temperature Phosphorescence in Organic Amorphous Materials under Ambient Conditions. Advanced Functional Materials, 2013, 23, 3386-3397.	7.8	643
3	Facile Synthesis of Marshmallowâ€like Macroporous Gels Usable under Harsh Conditions for the Separation of Oil and Water. Angewandte Chemie - International Edition, 2013, 52, 1986-1989.	7.2	408
4	Organic light emitters exhibiting very fast reverse intersystem crossing. Nature Photonics, 2020, 14, 643-649.	15.6	344
5	Triarylboronâ€Based Fluorescent Organic Lightâ€Emitting Diodes with External Quantum Efficiencies Exceeding 20 %. Angewandte Chemie - International Edition, 2015, 54, 15231-15235.	7.2	285
6	Photocontrolled Organocatalyzed Living Radical Polymerization Feasible over a Wide Range of Wavelengths. Journal of the American Chemical Society, 2015, 137, 5610-5617.	6.6	220
7	Versatile Indolocarbazoleâ€Isomer Derivatives as Highly Emissive Emitters and Ideal Hosts for Thermally Activated Delayed Fluorescent OLEDs with Alleviated Efficiency Rollâ€Off. Advanced Materials, 2018, 30, 1705406.	11.1	217
8	Transparent, Superflexible Doubly Cross-Linked Polyvinylpolymethylsiloxane Aerogel Superinsulators via Ambient Pressure Drying. ACS Nano, 2018, 12, 521-532.	7.3	211
9	Adamantyl Substitution Strategy for Realizing Solutionâ€Processable Thermally Stable Deepâ€Blue Thermally Activated Delayed Fluorescence Materials. Advanced Materials, 2018, 30, 1705641.	11.1	196
10	Polymethylsilsesquioxane–Cellulose Nanofiber Biocomposite Aerogels with High Thermal Insulation, Bendability, and Superhydrophobicity. ACS Applied Materials & Interfaces, 2014, 6, 9466-9471.	4.0	164
11	Visible-Light-Induced Reversible Complexation Mediated Living Radical Polymerization of Methacrylates with Organic Catalysts. Macromolecules, 2013, 46, 96-102.	2.2	159
12	Reversible Generation of a Carbon-Centered Radical from Alkyl Iodide Using Organic Salts and Their Application as Organic Catalysts in Living Radical Polymerization. Journal of the American Chemical Society, 2013, 135, 11131-11139.	6.6	154
13	Controlled emission colors and singlet–triplet energy gaps of dihydrophenazine-based thermally activated delayed fluorescence emitters. Journal of Materials Chemistry C, 2015, 3, 2175-2181.	2.7	147
14	Strategy for Designing Electron Donors for Thermally Activated Delayed Fluorescence Emitters. Journal of Physical Chemistry C, 2015, 119, 1291-1297.	1.5	137
15	Combined Inter―and Intramolecular Chargeâ€Transfer Processes for Highly Efficient Fluorescent Organic Lightâ€Emitting Diodes with Reduced Triplet Exciton Quenching. Advanced Materials, 2017, 29, 1606448.	11.1	131
16	Versatile Double-Cross-Linking Approach to Transparent, Machinable, Supercompressible, Highly Bendable Aerogel Thermal Superinsulators. Chemistry of Materials, 2018, 30, 2759-2770.	3.2	130
17	Reversible Complexation Mediated Living Radical Polymerization (RCMP) Using Organic Catalysts. Macromolecules, 2011, 44, 8709-8715.	2.2	125
18	A Superamphiphobic Macroporous Silicone Monolith with Marshmallowâ€like Flexibility. Angewandte Chemie - International Edition, 2013, 52, 10788-10791.	7.2	122

HIRONORI KAJI

#	Article	IF	CITATIONS
19	Highly Efficient Blue Electroluminescence Using Delayed-Fluorescence Emitters with Large Overlap Density between Luminescent and Ground States. Journal of Physical Chemistry C, 2015, 119, 26283-26289.	1.5	116
20	Fusion of Phosphole and 1,1′â€Biacenaphthene: Phosphorus(V)â€Containing Extended ï€â€Systems with High Electron Affinity and Electron Mobility. Angewandte Chemie - International Edition, 2011, 50, 8016-8020.	7.2	115
21	Superflexible Multifunctional Polyvinylpolydimethylsiloxaneâ€Based Aerogels as Efficient Absorbents, Thermal Superinsulators, and Strain Sensors. Angewandte Chemie - International Edition, 2018, 57, 9722-9727.	7.2	108
22	Reversible Thermal Recording Media Using Timeâ€Dependent Persistent Room Temperature Phosphorescence. Advanced Optical Materials, 2013, 1, 438-442.	3.6	101
23	Transparent, Highly Insulating Polyethyl- and Polyvinylsilsesquioxane Aerogels: Mechanical Improvements by Vulcanization for Ambient Pressure Drying. Chemistry of Materials, 2016, 28, 6860-6868.	3.2	96
24	Identification of Prime Factors to Maximize the Photocatalytic Hydrogen Evolution of Covalent Organic Frameworks. Journal of the American Chemical Society, 2020, 142, 9752-9762.	6.6	94
25	ï€-Extended Planarized Triphenylboranes with Thiophene Spacers. Organic Letters, 2013, 15, 6234-6237.	2.4	90
26	Blue organic light-emitting diodes realizing external quantum efficiency over 25% using thermally activated delayed fluorescence emitters. Scientific Reports, 2017, 7, 284.	1.6	88
27	Onâ€Top Ï€â€Stacking of Quasiplanar Molecules in Holeâ€Transporting Materials: Inducing Anisotropic Carrier Mobility in Amorphous Films. Angewandte Chemie - International Edition, 2014, 53, 5800-5804.	7.2	87
28	Gram-Scale Syntheses and Conductivities of [10]Cycloparaphenylene and Its Tetraalkoxy Derivatives. Journal of the American Chemical Society, 2017, 139, 18480-18483.	6.6	87
29	Enhanced Electroluminescence from a Thermally Activated Delayed-Fluorescence Emitter by Suppressing Nonradiative Decay. Physical Review Applied, 2015, 3, .	1.5	81
30	Highly Flexible Hybrid Polymer Aerogels and Xerogels Based on Resorcinol-Formaldehyde with Enhanced Elastic Stiffness and Recoverability: Insights into the Origin of Their Mechanical Properties. Chemistry of Materials, 2017, 29, 2122-2134.	3.2	76
31	Solid-State13C NMR Analyses of the Crystallineâ ``Noncrystalline Structure for Metallocene-Catalyzed Linear Low-Density Polyethylene. Macromolecules, 1997, 30, 7516-7521.	2.2	75
32	Comparative Study on the Structural, Optical, and Electrochemical Properties of Bithiopheneâ€Fused Benzo[<i>c</i>]phospholes. Chemistry - A European Journal, 2008, 14, 8102-8115.	1.7	75
33	Highly efficient electroluminescence from a solution-processable thermally activated delayed fluorescence emitter. Applied Physics Letters, 2015, 107, .	1.5	75
34	CP/MAS13C NMR Characterization of the Isomeric States and Intermolecular Packing in Tris(8-hydroxyquinoline) Aluminum(III) (Alq3). Journal of the American Chemical Society, 2006, 128, 4292-4297.	6.6	73
35	Effects of Porphyrin Substituents on Film Structure and Photoelectrochemical Properties of Porphyrin/Fullerene Composite Clusters Electrophoretically Deposited on Nanostructured SnO ₂ Electrodes. Chemistry - A European Journal, 2007, 13, 10182-10193.	1.7	70

36Acenaphtho[1, 2â€<i>c</i>]phosphole <i>P</i>â€Oxide: A Phosphole–Naphthalene Ï€â€Conjugated System with
High Electron Mobility. Chemistry - A European Journal, 2009, 15, 10000-10004.62

#	Article	IF	CITATIONS
37	Polymerization-induced phase separation in silica sol-gel systems containing formamide. Journal of Sol-Gel Science and Technology, 1993, 1, 35-46.	1.1	61
38	Highly Efficient Thermally Activated Delayed Fluorescence Emitters with a Small Singlet–Triplet Energy Gap and Large Oscillator Strength. Chemistry Letters, 2015, 44, 360-362.	0.7	57
39	Systematic Study on Alkyl Iodide Initiators in Living Radical Polymerization with Organic Catalysts. Macromolecules, 2014, 47, 6610-6618.	2.2	55
40	A light-emitting mechanism for organic light-emitting diodes: molecular design for inverted singlet–triplet structure and symmetry-controlled thermally activated delayed fluorescence. Journal of Materials Chemistry C, 2015, 3, 870-878.	2.7	51
41	Observation of spontaneous orientation polarization in evaporated films of organic light-emitting diode materials. Organic Electronics, 2018, 58, 313-317.	1.4	50
42	Percolation paths for charge transports in N,N′-diphenyl-N,N′-di(m-tolyl)benzidine (TPD). Organic Electronics, 2010, 11, 255-265.	1.4	49
43	Phenols and Carbon Compounds as Efficient Organic Catalysts for Reversible Chain Transfer Catalyzed Living Radical Polymerization (RTCP). Macromolecules, 2010, 43, 7971-7978.	2.2	49
44	Transparent Ethylene-Bridged Polymethylsiloxane Aerogels and Xerogels with Improved Bending Flexibility. Langmuir, 2016, 32, 13427-13434.	1.6	49
45	One- and Two-Dimensional Solid-State13C NMR Analyses of the Solid Structure and Molecular Motion of Poly(ε-caprolactone) Isothermally Crystallized from the Melt. Macromolecules, 1997, 30, 5791-5798.	2.2	48
46	Unveiling the Role of Langevin and Trap-Assisted Recombination in Long Lifespan OLEDs Employing Thermally Activated Delayed Fluorophores. ACS Applied Materials & Interfaces, 2019, 11, 1096-1108.	4.0	47
47	Exact Solution of Kinetic Analysis for Thermally Activated Delayed Fluorescence Materials. Journal of Physical Chemistry A, 2021, 125, 8074-8089.	1.1	47
48	Grafted Polymethylhydrosiloxane on Hierarchically Porous Silica Monoliths: A New Path to Monolith-Supported Palladium Nanoparticles for Continuous Flow Catalysis Applications. ACS Applied Materials & Interfaces, 2017, 9, 406-412.	4.0	46
49	Photoinduced Formation of Wrinkled Microstructures with Longâ€Range Order in Thin Oxide Films. Advanced Materials, 2007, 19, 4343-4346.	11.1	45
50	Highly efficient electroluminescence from purely organic donor–acceptor systems. Pure and Applied Chemistry, 2015, 87, 627-638.	0.9	45
51	Revealing bipolar charge-transport property of 4,4′-N,N′-dicarbazolylbiphenyl (CBP) by quantum chemical calculations. Organic Electronics, 2011, 12, 169-178.	1.4	44
52	Thermally Activated Delayed Fluorescent Materials Combining Intra- and Intermolecular Charge Transfers. ACS Applied Materials & amp; Interfaces, 2019, 11, 7192-7198.	4.0	44
53	Role of block copolymer surfactant on the pore formation in methylsilsesquioxane aerogel systems. RSC Advances, 2012, 2, 7166.	1.7	43
54	Intermolecular Packing in <i>B. mori</i> Silk Fibroin: Multinuclear NMR Study of the Model Peptide (Ala-Gly) ₁₅ Defines a Heterogeneous Antiparallel Antipolar Mode of Assembly in the Silk II Form. Macromolecules, 2015, 48, 28-36.	2.2	43

#	Article	IF	CITATIONS
55	Transparent Ethenylene-Bridged Polymethylsiloxane Aerogels: Mechanical Flexibility and Strength and Availability for Addition Reaction. Langmuir, 2017, 33, 4543-4550.	1.6	43
56	Manipulation of Charge-Transfer States by Molecular Design: Perspective from "Dynamic Exciton― Accounts of Materials Research, 2021, 2, 501-514.	5.9	42
57	Dynamic spring-back behavior in evaporative drying of polymethylsilsesquioxane monolithic gels for low-density transparent thermal superinsulators. Journal of Non-Crystalline Solids, 2016, 434, 115-119.	1.5	41
58	Enhancement of fluorescence in anthracene by chlorination: Vibronic coupling and transition dipole moment density analysis. Chemical Physics, 2014, 430, 47-55.	0.9	40
59	Highly Efficient and Stable Blue Organic Lightâ€Emitting Diodes based on Thermally Activated Delayed Fluorophor with Donorâ€Voidâ€Acceptor Motif. Advanced Science, 2022, 9, e2106018.	5.6	40
60	Solid-state 13C and 1H spin diffusion NMR analyses of the microfibril structure for bacterial cellulose. Solid State Nuclear Magnetic Resonance, 2003, 23, 198-212.	1.5	39
61	Electron–vibration interactions in carrier-transport material: Vibronic coupling density analysis in TPD. Chemical Physics Letters, 2008, 458, 152-156.	1.2	38
62	Solid-State 13C NMR Analyses for the Structure and Molecular Motion in the α Relaxation Temperature Region for Metallocene-Catalyzed Linear Low-Density Polyethylene. Macromolecules, 2000, 33, 4453-4462.	2.2	37
63	Relationship between room temperature phosphorescence and deuteration position in a purely aromatic compound. Chemical Physics Letters, 2014, 591, 119-125.	1.2	36
64	CP/MAS13C NMR Spectra of Frozen Solutions of Poly(vinyl alcohol) with Different Tacticities. Macromolecules, 1997, 30, 2519-2520.	2.2	35
65	In situ observation of phase separation processes in gelling alkoxy-derived silica system by light scattering method. Journal of Sol-Gel Science and Technology, 1994, 3, 169-188.	1.1	33
66	Rotational Motions in Atactic Poly(acrylonitrile) Studied by One- and Two-Dimensional15N Solid-State NMR and Dielectric Measurements. Macromolecules, 2003, 36, 6100-6113.	2.2	33
67	Comprehensive understanding of multiple resonance thermally activated delayed fluorescence through quantum chemistry calculations. Communications Chemistry, 2022, 5, .	2.0	33
68	Green- and blue-emitting tris(8-hydroxyquinoline) aluminum(III) (Alq3) crystalline polymorphs: Preparation and application to organic light-emitting diodes. Organic Electronics, 2012, 13, 2985-2990.	1.4	32
69	Highly efficient solution-processed host-free organic light-emitting diodes showing an external quantum efficiency of nearly 18% with a thermally activated delayed fluorescence emitter. Applied Physics Express, 2016, 9, 032102.	1.1	32
70	Low-density, transparent aerogels and xerogels based on hexylene-bridged polysilsesquioxane with bendability. Journal of Sol-Gel Science and Technology, 2017, 81, 42-51.	1.1	32
71	CP/MAS13C NMR analyses of hydrogen bonding and the chain conformation in the crystalline and noncrystalline regions for poly(vinyl alcohol) films. Journal of Polymer Science, Part B: Polymer Physics, 2000, 38, 1-9.	2.4	31
72	Conformation and Dynamics of Atactic Poly(acrylonitrile). 1. Trans/Gauche Ratio from Double-Quantum Solid-State13C NMR of the Methylene Groups. Macromolecules, 2000, 33, 5169-5180.	2.2	31

#	Article	IF	CITATIONS
73	Conformation and Dynamics of Atactic Poly(acrylonitrile). 2. Torsion Angle Distributions in Meso Dyads from Two-Dimensional Solid-State Double-Quantum 13C NMR. Macromolecules, 2001, 34, 7368-7381.	2.2	31
74	Relationships between Light-Emitting Properties and Different Isomers in Polymorphs of Tris(8-hydroxyquinoline) Aluminum(III) (Alq3) Analyzed by Solid-State27Al NMR and Density Functional Theory (DFT) Calculations. Japanese Journal of Applied Physics, 2005, 44, 3706-3711.	0.8	31
75	Determination of Accurate ¹ H Positions of (Ala-Gly)n as a Sequential Peptide Model of Bombyx mori Silk Fibroin before Spinning (Silk I). Macromolecules, 2013, 46, 8046-8050.	2.2	31
76	Living Radical Polymerization via Organic Superbase Catalysis. Polymers, 2014, 6, 860-872.	2.0	31
77	Crystallineâ^'Noncrystalline Structure and Chain Diffusion Associated with the 180° Flip Motion for Polyethylene Single Crystals As Revealed by Solid-State13C NMR Analyses. Macromolecules, 2000, 33, 7093-7100.	2.2	30
78	A boron-containing molecule as an efficient electron-transporting material with low-power consumption. Applied Physics Letters, 2010, 97, 142111.	1.5	30
79	Band-like Transport of Charge Carriers in Oriented Two-Dimensional Conjugated Covalent Organic Frameworks. Chemistry of Materials, 2022, 34, 736-745.	3.2	30
80	Formation of porous gel morphology by phase separation in gelling alkoxy-derived silica. Affinity between silica polymers and solvent Journal of Non-Crystalline Solids, 1995, 181, 16-26.	1.5	29
81	Detailed analysis of charge transport in amorphous organic thin layer by multiscale simulation without any adjustable parameters. Scientific Reports, 2016, 6, 39128.	1.6	29
82	Theoretical design of a hole-transporting molecule: hexaaza[16]parabiphenylophane. Journal of Materials Chemistry, 2011, 21, 6375.	6.7	28
83	Ultrahigh Power Efficiency Thermally Activated Delayed Fluorescent OLEDs by the Strategic Use of Electronâ€Transport Materials. Advanced Optical Materials, 2018, 6, 1800376.	3.6	28
84	Solid-State13C NMR Analyses of the Structure and Chain Conformation of Thermotropic Liquid Crystalline Polyurethane Crystallized from the Melt through the Liquid Crystalline State. Macromolecules, 1997, 30, 5799-5803.	2.2	27
85	Selective Observation and Quantification of Amorphous Trans Conformers in Doubly13C-Labeled Poly(ethylene terephthalate), PET, by Zero-Quantum Magic-Angle-Spinning Solid-State NMR. Macromolecules, 2002, 35, 7993-8004.	2.2	27
86	Refined Crystal Structure of <i>Samia cynthia ricini</i> Silk Fibroin Revealed by Solid-State NMR Investigations. Biomacromolecules, 2017, 18, 1965-1974.	2.6	27
87	Macromolecular Architectures Designed by Living Radical Polymerization with Organic Catalysts. Polymers, 2014, 6, 311-326.	2.0	26
88	Determination of accurate 1H positions of an alanine tripeptide with anti-parallel and parallel β-sheet structures by high resolution 1H solid state NMR and GIPAW chemical shift calculation. Chemical Communications, 2012, 48, 11199.	2.2	25
89	Refined Structure Determination of Blue-Emitting Tris(8-hydroxyquinoline) Aluminum(III) (Alq ₃) by the Combined Use of Cross-Polarization/Magic-Angle Spinning ¹³ C Solid-State NMR and First-Principles Calculation. Journal of Physical Chemistry C, 2013, 117, 18809-18817.	1.5	25
90	Boehmite Nanofiber–Polymethylsilsesquioxane Core–Shell Porous Monoliths for a Thermal Insulator under Low Vacuum Conditions. Chemistry of Materials, 2016, 28, 3237-3240.	3.2	25

HIRONORI KAJI

#	Article	IF	CITATIONS
91	Formation of porous gel morphology by phase separation in gelling alkoxy-derived silica. Phenomenological study. Journal of Non-Crystalline Solids, 1995, 185, 18-30.	1.5	24
92	Difference in the structures of alanine tri―and tetraâ€peptides with antiparallel βâ€sheet assessed by Xâ€ray diffraction, solidâ€state NMR and chemical shift calculations by GIPAW. Biopolymers, 2014, 101, 13-20.	1.2	24
93	Noise Reduction in Solid-State NMR Spectra Using Principal Component Analysis. Journal of Physical Chemistry A, 2019, 123, 10333-10338.	1.1	24
94	Multiscale simulation of charge transport in a host material, N,N′-dicarbazole-3,5-benzene (mCP), for organic light-emitting diodes. Journal of Materials Chemistry C, 2015, 3, 5549-5555.	2.7	23
95	Synthesis of high-silica and low-silica zeolite monoliths with trimodal pores. Microporous and Mesoporous Materials, 2010, 132, 538-542.	2.2	22
96	A designed fluorescent anthracene derivative: Theory, calculation, synthesis, and characterization. Chemical Physics Letters, 2014, 602, 80-83.	1.2	22
97	Increasing the horizontal orientation of transition dipole moments in solution processed small molecular emitters. Journal of Materials Chemistry C, 2017, 5, 6555-6562.	2.7	22
98	[Paper] Meta-linking Strategy for Thermally Activated Delayed Fluorescence Emitters with a Small Singlet-Triplet Energy Gap. ITE Transactions on Media Technology and Applications, 2015, 3, 108-113.	0.3	21
99	Effects of Structural and Energetic Disorders on Charge Transports in Crystal and Amorphous Organic Layers. Scientific Reports, 2018, 8, 5203.	1.6	21
100	Parameter-Free Multiscale Simulation Realising Quantitative Prediction of Hole and Electron Mobilities in Organic Amorphous System with Multiple Frontier Orbitals. Scientific Reports, 2018, 8, 13462.	1.6	21
101	Ambient-dried highly flexible copolymer aerogels and their nanocomposites with polypyrrole for thermal insulation, separation, and pressure sensing. Polymer Chemistry, 2019, 10, 4980-4990.	1.9	21
102	Efficient blue thermally activated delayed fluorescence emitters showing very fast reverse intersystem crossing. Applied Physics Express, 2021, 14, 071003.	1.1	21
103	Conformation and Dynamics of Atactic Poly(acrylonitrile). 3. Characterization of Local Structure by Two-Dimensional 2Hâ^'13C Solid-State NMR. Macromolecules, 2001, 34, 7382-7391.	2.2	20
104	A combined experimental and theoretical study of the conformation of N,N′-diphenyl-N,N′-di(m-tolyl)benzidine using solid-state 15N NMR and DFT calculations. Chemical Physics Letters, 2005, 401, 246-253.	1.2	19
105	Electron–vibration interactions in triphenylamine cation: Why are triphenylamine-based molecules good hole-transport materials?. Chemical Physics Letters, 2010, 486, 130-136.	1.2	19
106	Lamellar Structure in Alanine–Glycine Copolypeptides Studied by Solid-State NMR Spectroscopy: A Model for the Crystalline Domain of <i>Bombyx mori</i> Silk Fibroin in Silk II Form. Biomacromolecules, 2020, 21, 3102-3111.	2.6	19
107	One- and Two-Dimensional MAS 13C NMR Analyses of Molecular Motions in Poly(2-hydroxypropyl Ether) Tj ETQq	1 1 0.7843 2.2	314 rgBT /0 18
108	Impact of the position of the imine linker on the optoelectronic performance of π-conjugated organic frameworks. Molecular Systems Design and Engineering, 2019, 4, 325-331.	1.7	18

#	Article	IF	CITATIONS
109	Thermally Activated Delayed Fluorescence Benzyl Cellulose Derivatives for Nondoped Organic Light-Emitting Diodes. Macromolecules, 2020, 53, 2864-2873.	2.2	18
110	Effect of Vibronic Coupling on Correlated Triplet Pair Formation in the Singlet Fission Process of Linked Tetracene Dimers. Journal of Physical Chemistry A, 2020, 124, 3641-3651.	1.1	18
111	Characterization of local structures in amorphous and crystalline tris(8-hydroxyquinoline) aluminum(III) (Alq3) by solid-state 27Al MQMAS NMR spectroscopy. Chemical Physics Letters, 2009, 471, 80-84.	1.2	17
112	Phase separation kinetics in silica sol-gel system containing polyethylene oxide. I. Initial stage. Journal of Sol-Gel Science and Technology, 1994, 2, 227-231.	1.1	16
113	Solid-State 13C NMR and 1H CRAMPS Investigations of the Hydration Process and Hydrogen Bonding for Poly(vinyl alcohol) Films. Polymer Journal, 2001, 33, 356-363.	1.3	16
114	Structure and crystallization of sub-elementary fibrils of bacterial cellulose isolated by using a fluorescent brightening agent. Cellulose, 2012, 19, 713-727.	2.4	16
115	Superflexible Multifunctional Polyvinylpolydimethylsiloxaneâ€Based Aerogels as Efficient Absorbents, Thermal Superinsulators, and Strain Sensors. Angewandte Chemie, 2018, 130, 9870-9875.	1.6	16
116	Patterning of hybrid titania film using photopolymerization. Thin Solid Films, 2004, 466, 48-53.	0.8	15
117	Characterization of Carbon Filler Distribution Ratio in Polyisoprene/Polybutadiene Rubber Blends by High-Resolution Solid-State13C NMR. Macromolecules, 2007, 40, 9451-9454.	2.2	15
118	Theoretical Determination of Rate Constants from Excited States: Application to Benzophenone. Journal of Physical Chemistry A, 2021, 125, 9000-9010.	1.1	15
119	A multifunctional hole-transporter for high-performance TADF OLEDs and clarification of factors governing the transport property by multiscale simulation. Journal of Materials Chemistry C, 2022, 10, 8694-8701.	2.7	15
120	Two-Dimensional13C Magic Angle Turning NMR Analyses of Dynamics in Poly(2-hydroxypropyl ether of) Tj ETQq0	0.0.rgBT 2.2	/Overlock 10 14
121	Solid-state nuclear magnetic resonance analysis of phase separation behavior of regioregular poly(3-hexylthiophene) and [6,6]-phenyl-C61-butyric acid methyl ester in bulk heterojunction organic solar cells. Applied Physics Letters, 2011, 99, .	1.5	14
122	Analysis of Molecular Orientation in Organic Semiconducting Thin Films Using Static Dynamic Nuclear Polarization Enhanced Solid‧tate NMR Spectroscopy. Angewandte Chemie - International Edition, 2017, 56, 14842-14846.	7.2	14
123	Efficient Direct Reverse Intersystem Crossing between Charge Transferâ€Type Singlet and Triplet States in a Purely Organic Molecule. ChemPhysChem, 2021, 22, 625-632.	1.0	14
124	Solid-state NMR analyses of the structure and dynamics of polymers in the different states. Journal of Molecular Structure, 1998, 441, 303-311.	1.8	13
125	Studies on Different Types of Hydrogen Bonds in Poly(vinyl alcohol) Films by 1H CRAMPS and Solid-State Two-Dimensional 1H-13C Heteronuclear Correlation Analyses. Polymer Journal, 2001, 33, 190-198.	1.3	13
126	Vibronic coupling density analysis of hole-transporting materials: Electron-density difference in DFT and HF methods. Organic Electronics, 2010, 11, 1277-1287.	1.4	13

#	Article	IF	CITATIONS
127	The Influence of Quasiplanar Structures of Partially Oxygen-Bridged Triphenylamine Dimers on the Properties of Their Bulk Films. Bulletin of the Chemical Society of Japan, 2016, 89, 726-732.	2.0	13
128	Molecular dynamics and orientation of stretched rubber by solid-state 13C NMR. Polymer Journal, 2010, 42, 25-30.	1.3	12
129	Reversible Complexation Mediated Polymerization (RCMP) of Methyl Methacrylate. ACS Symposium Series, 2012, , 305-315.	0.5	12
130	Theoretical Estimation of the Chemical Effect on K X-Ray Intensity Ratios for 4d Elements. X-Ray Spectrometry, 1997, 26, 269-271.	0.9	11
131	Analyses of the local order in poly(ethylene terephthalate) in the glassy state by two-dimensional solid-state 13C spin diffusion nuclear magnetic resonance spectroscopy. Journal of Chemical Physics, 1998, 109, 4651-4658.	1.2	11
132	Superheated Melting Kinetics of Metastable Chain-Folded Polymer Crystals. Crystal Growth and Design, 2018, 18, 3637-3643.	1.4	11
133	Tris(triazolo)triazine-based emitters for solution-processed blue thermally activated delayed fluorescence organic light-emitting diodes. Materials Advances, 2020, 1, 2862-2871.	2.6	11
134	Molecular Vibration Accelerates Charge Transfer Emission in a Highly Twisted Blue Thermally Activated Delayed Fluorescence Material. Journal of Physical Chemistry A, 2021, 125, 4534-4539.	1.1	11
135	Modification of nanometer range pores in silica gels with interconnected macropores by solvent exchange. Journal of Non-Crystalline Solids, 1992, 145, 80-84.	1.5	10
136	1H CRAMPS Measurements of Different Types of OH Groups in Poly(vinyl alcohol) Films. Polymer Journal, 1999, 31, 105-107.	1.3	10
137	Rheology of Living Bifunctional Polybutadienyl Dilithium Chains in Benzene:Viscoelastic Evaluation of Aggregate Lifetime. Macromolecules, 2003, 36, 220-228.	2.2	10
138	Solid-state 13C NMR investigation of the structure and dynamics of highly drawn polyethylene—detection of the oriented non-crystalline component. Polymer, 2006, 47, 2470-2481.	1.8	10
139	Fabrication of hydrophobic polymethylsilsesquioxane aerogels by a surfactant-free method using alkoxysilane with ionic group. Journal of Asian Ceramic Societies, 2017, 5, 104-108.	1.0	10
140	Kinetics of "Melting―of Sucrose Crystals. Crystal Growth and Design, 2018, 18, 2602-2608.	1.4	10
141	Near-Unity Singlet Fission on a Quantum Dot Initiated by Resonant Energy Transfer. Journal of the American Chemical Society, 2021, 143, 17388-17394.	6.6	10
142	Chemical effect on the K X-ray intensity ratios for 4d transition metals. Physics Letters, Section A: General, Atomic and Solid State Physics, 1986, 118, 44-46.	0.9	9
143	Investigation of Dynamics of Poly(dimethylsilane) in the Mesophase by Solid-State 29Si NMR:  Evidence for Rotator Phase. Macromolecules, 2007, 40, 5420-5423.	2.2	9
144	Vibronic coupling density analysis for the chain-length dependence of reorganization energies in oligofluorenes: a comparative study with oligothiophenes. Physical Chemistry Chemical Physics, 2013, 15, 14006.	1.3	9

#	Article	IF	CITATIONS
145	Thermally Activated Delayed Fluorescence Emitter with a Symmetric Acceptor-Donor-Acceptor Structure. Journal of Photopolymer Science and Technology = [Fotoporima Konwakai Shi], 2017, 30, 475-481.	0.1	9
146	Studies of the Phase Transitions, Structure, and Dynamics for Main-Chain Thermotropic Liquid Crystalline Polyethers and Polyurethanes with the Same Mesogen and Spacer Units. Macromolecules, 2003, 36, 4160-4167.	2.2	8
147	Solid-State 13C NMR Studies of the Structure and Chain Conformation of Thermotropic Liquid Crystalline Polyether Crystallized from the Liquid Crystalline Glassy Phase. Polymer Journal, 2004, 36, 403-412.	1.3	8
148	Enhanced hole injection in organic light-emitting diodes by optimized synthesis of self-assembled monolayer. Organic Electronics, 2011, 12, 1600-1605.	1.4	8
149	Local stoichiometry in amorphous supramolecular composites analyzed by solid-state C13 nuclear magnetic resonance. Applied Physics Letters, 2011, 98, 113301.	1.5	8
150	Solutionâ€processable thermally activated delayed fluorescence emitters for application in organic light emitting diodes. Journal of the Society for Information Display, 2017, 25, 480-485.	0.8	8
151	Dynamics of Monofunctional Polybutadienyl Lithium Chains Aggregated in Benzene. Polymer Journal, 2006, 38, 277-288.	1.3	7
152	Planarity of triphenylamine moieties of a typical hole-transport material for OLEDs, N,N′-diphenyl-N,N′-di(m-tolyl)benzidine (TPD), in the amorphous state. Journal of Molecular Structure, 2009, 927, 82-87.	1.8	7
153	Sensitivity boosting in solid-state NMR of thin organic semiconductors by a paramagnetic dopant of copper phthalocyanine. Chemical Physics Letters, 2013, 556, 195-199.	1.2	7
154	Material degradation of liquid organic semiconductors analyzed by nuclear magnetic resonance spectroscopy. AIP Advances, 2015, 5, 087124.	0.6	7
155	Conformation Control of Iminodibenzyl-Based Thermally Activated Delayed Fluorescence Material by Tilted Face-to-Face Alignment With Optimal Distance (tFFO) Design. Frontiers in Chemistry, 2020, 8, 530.	1.8	7
156	Characterization of Molecular Orientation of Stretched Natural Rubber by Solid-State 13C NMR. Polymer Journal, 2007, 39, 502-503.	1.3	6
157	The effect of gas emission on the strength of composite products derived using alkali-activated municipal solid waste incineration fly ash/pyrophyllite-based systems. Chemosphere, 2019, 228, 513-520.	4.2	6
158	Acceleration of Reverse Intersystem Crossing using Different Types of Charge Transfer States. Chemistry - an Asian Journal, 2021, 16, 1073-1076.	1.7	6
159	Clarification of isomeric structures and the effect of intermolecular interactions in blue-emitting aluminum complex Alq3 using first-principles 27Al NMR calculations. Chemical Physics Letters, 2014, 605-606, 1-4.	1.2	5
160	Organic Electroluminescent Materials Realizing Efficient Conversion from Electricity to Light. Journal of Photopolymer Science and Technology = [Fotoporima Konwakai Shi], 2016, 29, 305-310.	0.1	5
161	Multichromophore Molecular Design for Thermally Activated Delayed-Fluorescence Emitters with Near-Unity Photoluminescence Quantum Yields. Journal of Organic Chemistry, 2021, 86, 11531-11544.	1.7	5
162	Imidazole Acceptor for Both Vacuum-Processable and Solution-Processable Efficient Blue Thermally Activated Delayed Fluorescence. ACS Omega, 0, , .	1.6	5

#	Article	IF	CITATIONS
163	Formation of the Liquid Crystalline Glassy Phase and Cold Crystallization of a New Crystal Form from the Glassy Phase for Thermotropic Liquid Crystalline Polyether. Polymer Journal, 2003, 35, 951-959.	1.3	4
164	Living Radical Polymerizations Using Sodium Iodide and Potassium Iodide as Catalysts. ACS Symposium Series, 2015, , 171-182.	0.5	4
165	Aerogels from Chloromethyltrimethoxysilane and Their Functionalizations. Langmuir, 2017, 33, 13841-13848.	1.6	4
166	Dipole Moment in the Excited State: An Important Property for TADF Hosts. CheM, 2018, 4, 2018-2019.	5.8	4
167	Exploring the capability of mayenite (12CaO·7Al2O3) as hydrogen storage material. Scientific Reports, 2021, 11, 6278.	1.6	4
168	Sine-modulated two-dimensional pure exchange solid-state NMR as a tool for characterizing dynamics in solids. Chemical Physics Letters, 2003, 377, 322-328.	1.2	3
169	Vibronic interactions in hole-transporting molecules: An interplay with electron–hole interactions. Chemical Physics Letters, 2011, 507, 151-156.	1.2	3
170	Living Radical Polymerizations with Organic Catalysts. RSC Polymer Chemistry Series, 2013, , 250-286.	0.1	3
171	Distribution ratio of carbon black in polyisobutyrene/polyisoprene rubber blends using high-resolution solid-state 13C NMR. Polymer Journal, 2015, 47, 422-427.	1.3	3
172	Synthesis and characterization of cyclic P3HT as a donor polymer for organic solar cells. Journal of Polymer Science, Part B: Polymer Physics, 2019, 57, 266-271.	2.4	3
173	Correlated Triplet Pair Formation Activated by Geometry Relaxation in Directly Linked Tetracene Dimer (5,5′-Bitetracene). ACS Omega, 2021, 6, 2638-2643.	1.6	3
174	Pionic X-ray intensity ratios in chromium compounds. Journal of Radioanalytical and Nuclear Chemistry, 1989, 135, 207-213.	0.7	2
175	Solid-State 13C NMR Analysis of the Crystalline–Noncrystalline Structure and Chain Conformation of Thermotropic Liquid Crystalline Polyester. Polymer Journal, 2004, 36, 830-840.	1.3	2
176	Relationship between Resistivity and Structure of Photosensitive Organic Silsesquioxanes by Impedance Spectroscopy and Solid-State29Si Nuclear Magnetic Resonance. Japanese Journal of Applied Physics, 2008, 47, 1377-1381.	0.8	2
177	Theoretical design for carrier-transporting molecules in view of vibronic couplings. Journal of Photonics for Energy, 2012, 2, 021201 Vibronic couplings in <mm:math <="" altimg="si21.gif" overflow="scroll" td=""><td>0.8</td><td>2</td></mm:math>	0.8	2
178	xmlns:xocs="http://www.elsevier.com/xml/xocs/dtd" xmlns:xs="http://www.w3.org/2001/XMLSchema" xmlns:xsi="http://www.w3.org/2001/XMLSchema-instance" xmlns="http://www.elsevier.com/xml/ja/dtd" xmlns:ja="http://www.elsevier.com/xml/ja/dtd" xmlns:mml="http://www.w3.org/1998/Math/MathML" xmlns:tb="http://www.elsevier.com/xml/common/table/dtd"	1.2	2
179	xmlns:sb="http://www.elsevier.com/xml/common/struct-bib/dtd" xmlns:ce="http://www.elsevier.com/x Visual Understanding of Vibronic Coupling and Quantitative Rate Expression for Singlet Fission in Molecular Aggregates. Bulletin of the Chemical Society of Japan, 2020, 93, 1305-1313.	2.0	2
180	Improving NIR sensor detectivity of BODIPY/C60 bulk heterojunction photodiode. Japanese Journal of Applied Physics, 2020, 59, SGGG04.	0.8	2

#	Article	IF	CITATIONS
181	Thiopheneâ€Fused Naphthodiphospholes: Modulation of the Structural and Electronic Properties of Polycyclic Aromatics by Precise Fusion of Heteroles. ChemPlusChem, 2021, 86, 130-136.	1.3	2
182	Comprehensive study on operational lifetime of organic light-emitting diodes: effects of molecular structure and energy transfer. Japanese Journal of Applied Physics, 2021, 60, 040902.	0.8	2
183	Truxenone Triimide: Twoâ€Dimensional Molecular Arrangements of Triangular Molecules for Air Stable nâ€Type Semiconductors. Advanced Electronic Materials, 0, , 2101390.	2.6	2
184	An Analytical Expression of Magic Angle Spinning Nuclear Magnetic Resonance Free Induction Decay in Two-Site Exchange Problem. Chinese Physics Letters, 1998, 15, 453-454.	1.3	1
185	Geometric and electronic structures of a hole-transport material, TPD, and related materials studied by DFT calculations and solid-state NMR. Proceedings of SPIE, 2008, , .	0.8	1
186	"114â€â€Type Nitrides LnAl(Si _{4â°'<i>x</i>} Al _{<i>x</i>})N ₇ O _{<i>î^</i>} with Unusual [AlN ₆] Octahedral Coordination. Angewandte Chemie - International Edition, 2017, 56, 3886-3891.	7.2	1
187	Analysis of Molecular Orientation in Organic Semiconducting Thin Films Using Static Dynamic Nuclear Polarization Enhanced Solid‧tate NMR Spectroscopy. Angewandte Chemie, 2017, 129, 15038-15042.	1.6	1
188	Carbazole and Benzophenone Based Twisted Donor–Acceptor Systems as Solution Processable Green Thermally Activated Delayed Fluorescence Organic Light Emitters. Chemistry Letters, 2018, 47, 1236-1239.	0.7	1
189	Synthesis and Characterization of 5,5 \hat{a} € ² -Bitetracene. Chemistry Letters, 2021, 50, 800-803.	0.7	1
190	25â€1: <i>Invited Paper:</i> Multiscale Charge Transport Simulation and <i>in silico</i> Material Design for Highlyâ€Efficient OLEDs. Digest of Technical Papers SID International Symposium, 2021, 52, 308-311.	0.1	1
191	Effect of a twin-emitter design strategy on a previously reported thermally activated delayed fluorescence organic light-emitting diode. Beilstein Journal of Organic Chemistry, 2021, 17, 2894-2905.	1.3	1
192	Near-infrared-red-orange thermally activated delayed fluorescence emitters using a strong tetracoordinated difluoroboronated acceptor. Japanese Journal of Applied Physics, 0, , .	0.8	1
193	Origin of the different emission wavelengths in Alq 3 analyzed by solid-state NMR. Proceedings of SPIE, 2007, , .	0.8	Ο
194	Living Radical Polymerizations with Organic Catalysts. Kobunshi Ronbunshu, 2011, 68, 223-231.	0.2	0
195	Investigation of aggregated structures in organic light-emitting diodes: approach from solid-state NMR. , 2012, , .		Ο
196	Degradation of blue phosphorescent organic LEDs analyzed by solution NMR spectroscopy. Proceedings of SPIE, 2014, , .	0.8	0
197	Organic light-emitting diodes: multiscale charge transport simulation and fabrication of new thermally activated delayed fluorescence (TADF) materials. , 2015, , .		0
198	Efficient Direct Reverse Intersystem Crossing between Charge Transferâ€Type Singlet and Triplet States in a Purely Organic Molecule. ChemPhysChem, 2021, 22, 621-621.	1.0	0

#	Article	IF	CITATIONS
199	In silico Discovery of Emitters and Charge Transporters for Organic Light-Emitting Diodes. , 2019, , .		ο
200	<i>N</i> -Adamantylphthalimide-based Thermally Activated Delayed Fluorescence Emitter for Solution-processed Organic Light-emitting Diodes. Chemistry Letters, 2021, 50, 1953-1955.	0.7	0